Supporting Information

Truss bridge-like anhydrous stacking in hybrid crystal triggers ultra-high stability and robust birefringence

Ping Wang,[a] Qiya Huang,[a] Xiaoli Meng,[a] Lehui Liu,[b] Qi Wu,*[c] Hongming Liu*[a]

[a] *Guangxi Key Laboratory of Electrochemical Energy Materials, Guangxi Colleges and Universities Key Laboratory of Applied Chemistry Technology and Resource Development, School of Chemistry and Chemical Engineering, Guangxi University, Nanning, Guangxi 530004, China. E-mail: hongming9224@126.com*

[b] *Key Laboratory of Optoelectronic Materials Chemistry and Physics, Fujian Institute of Research on the Structure of Matter, Chinese Academy of Sciences, Fujian, Fuzhou, 350002, China*

[c] *State Key Laboratory of New Textile Materials and Advanced Processing, Wuhan Textile University, Wuhan, Hubei 430200, China. E-mail: wuqi2011@whu.edu.cn*

1. Experimental Section

Experimental Procedures

Reagents. The starting materials used in the synthetic process include terephthalic acid ($C_8H_6O_4$, TPA) (Maclin), NaOH (AR, a reagent from Sinopharm Chemical), KOH (AR, a reagent from Sinopharm Chemical), and RbOH (AR, a reagent from Sinopharm Chemical). All raw materials are from commercial sources and do not require further purification before use.

Synthesis. Crystals of TPANa, TPAK and TPARb were synthesized through hydrothermal reactions at moderate temperatures. The mixture of NaOH (8 mmol)/KOH (4 mmol)/RbOH (4 mmol), $C_8H_6O_4$ (1 mmol) and deionized water (2 mL) was placed in an autoclave lined with polytetrafluoroethylene, heated to 140 ˚C and maintained for 48 hours. Then cool at a rate of 3 ˚C/h to the ambient temperature. The reaction products were washed with anhydrous ethanol and dried at room temperature to separate colorless and transparent plate-like crystals (Fig. S1), with a yield of approximately 60−78 %.

Measurements

Powder X-ray Diffraction (PXRD)

PXRD patterns were collected on a Rigaku D/MAX 2500V diffractometer equipped with Cu k_α radiation (λ=1.540598 Å), in the angular range of 2ϑ from 10° to 70°, with a scan rate of 1 °/min at room temperature.

X-ray Photoelectron Spectroscopy (XPS)

XPS was obtained using the Thermo Scientific Nexsa X-ray photoelectron spectrometer from the United States, and the binding energy of the C 1s peak at 284.8 eV was used as the energy standard.

Energy Dispersive X-Ray Spectroscopy (EDS)

Energy-dispersive X-ray spectrometry was performed on a Zeiss Sigma 300 field-emission scanning electron microscope equipped with an X-ray spectroscope (15 kV).

Thermal analysis

The thermal stability was measured on a Netzsch STA 449F3 thermal analyzer instrument. About 10 mg of powders were placed in an alumina crucible and heated from 25 to 800 °C at a heating rate of 10 °C/min in an N_2 shielding atmosphere.

UV–Vis–NIR spectrum

UV-vis-NIR spectrophotometer (equipped with an integrating sphere) was used to record UV-vis reflectance data in the spectral range of 200−800 nm, with spectrographically pure $BaSO_4$ served as the reference substance, and the *Kubelka-Munk* function: $F(R)=(1-R)^2/2R$, where R is the reflectance.[1] was applied to convert the reflectance spectrum into the absorption spectrum.

Infrared (IR) spectrum

The powder IR spectrum of the polycrystalline samples was recorded using a Nicolet iS10 Fourier transform IR spectrometer within the wavenumber range of 4000-500 cm^{-1} at room temperature.

Birefringence Measurements

The birefringence measurement was performed on a Mshot MP41 cross-polarization microscope

with a visible light source, and the specific optical path difference can be determined by matching the Michel Le'vy chart.[2] The birefringence index (Δn) of a crystal can be obtained using the following formula: $\Delta R = \Delta n \times T$ (ΔR, optical path difference; T, crystal thickness).

Single-Crystal X-ray Diffraction (XRD)

Data collections for the compound were executed on a Bruker SMARTAPEXDUO diffractometer with graphite-monochromated Mo-Kα radiation (λ =0.71073 Å) at 296 (2)K. Data set reduction and integration were accomplished using the SAINTPLUS19 crystallographic software package. The SHELXTL software package[3] was utilized to directly process and refine the structure, and structural refinement was performed using the Olex2 software.[4] After refining several times, reasonable R values were gained, and the formula of the compound was determined to be $Na_2(C_8H_4O_4)$ (TPANa), $K_2(C_8H_4O_4)$ (TPAK) and $Rb_2(C_8H_4O_4)\cdot 2H_2O$ (TPARb). The space group was checked with PLATON[5] program and no higher symmetry was found. Table S1 summarizes the relevant crystal data and structural refinement information for TPANa,TPAK and TPARb. The details of the crystal structure (CCDC 2503104-2503106) can be sought from the Cambridge Crystallographic Data Centre at www.ccdc.cam.ac.uk/data_request/cif.

Computational Methods

First-principles calculations were carried out using the CASTEP [6] package based on density-functional theory (DFT).[7,8] Simulated band structures, electron localization function (ELF), density of states (DOS), and optical properties for compounds TPANa, TPAK and TPARb were computed using the Perdew–Burke–Ernzerhof (PBE) generalized gradient approximation (GGA) and normconserving pseudopotentials. The kinetic energy cutoff was set to 750 eV for TPANa, TPAK and TPARb, and the Monkhorst−Pack k-point meshes were set to be less than 0.04 $Å^{-1}$.[9]

To obtain the linear optical properties, the complex dielectric function $\varepsilon(\omega) = \varepsilon_1(\omega) + i\varepsilon_2(\omega)$ has been determined in the random phase approximation from the PBE wavefunctions. The imaginary part of the dielectric function due to direct inter-band transitions is given by the expression,

$$\varepsilon_2(\mathrm{h}\omega) = \frac{2e^2\pi}{\Omega\varepsilon_0}\sum_{k,v,c}\left|\left\langle\psi_k^c\left|u\cdot r\right|\psi_k^v\right\rangle\right|^2\delta(E_k^c - E_k^v - E)$$

where Ω, ω, u, v and c are the unit-cell volume, photon frequencies, the vector defining the polarization of the incident electric field, valence and conduction bands, respectively. The real part of the dielectric function is obtained from ε_2 by a Kramers-Kronig transformation,

$$\varepsilon_1(\omega) = 1 + (\frac{2}{\pi})\int_0^{+\infty} d\omega' \frac{\omega'^2\varepsilon_2(\omega)}{\omega'^2 - \omega^2}$$

2. Supporting Tables and Figures

Table S1. Crystal data and structure refinement for TPANa, TPAK, TPARb.

Identification code	TPANa	TPAK	TPARb
Empirical formula	$C_8H_4O_4Na_2$	$C_8H_4O_4K_2$	$C_8H_8O_6Rb_2$
Formula weight	210.09	242.31	371.08
Temperature	301(2) K	298(2) K	298(2) K
Wavelength	0.71073 Å	0.71073 Å	0.71073 Å
Crystal system	Monoclinic	Monoclinic	Monoclinic
Space group	$P2_1/c$	$P2_1/c$	$P2_1/c$
Unit cell dimensions	a = 19.7373(8) Å	a = 10.5503(7) Å	a = 12.6482(8) Å
	b = 3.54730(10) Å	b = 3.9330(2) Å	b = 3.95200(10) Å
	c = 10.8108(5) Å	c = 11.5147(8) Å	c = 11.8388(7) Å
	b = 105.844(4) °	b = 113.066(8)°	b= 111.880(7)°
Volume	728.15(5) Å^3	439.60(5) Å^3	549.14(6) Å^3
Z	4	2	2
Density (calculated)	1.916 g/cm^3	1.831 g/cm^3	2.244 g/cm^3
Absorption coefficient	0.251 mm^{-1}	1.058 mm^{-1}	8.920 mm^{-1}
F(000)	424	244	356
Reflections collected	8322	3312	4625
Independent reflections	1696 [R(int) = 0.0311]	980 [R(int) = 0.0285]	1238 [R(int) = 0.0285]
Completeness to theta = 25.242°	99.5 %	100.0 %	100.0 %
Goodness-of-fit on F^2	1.144	1.114	1.082
Final R indices [I>2sigma(I)]	R1 = 0.0477, wR_2 = 0.1136	R1 = 0.0289, wR_2 = 0.0637	R1 = 0.0237, wR_2 = 0.0514
R indices (all data)	R1 = 0.0546, wR_2 = 0.1169	R1 = 0.0354, wR_2 = 0.0674	R1 = 0.0344, wR_2 = 0.0534

Table S2. Atomic coordinates ($\times 10^4$) and equivalent isotropic displacement parameters ($Å^2 \times 10^2$) for TPANa. U_{eq} is defined as one third of the trace of the orthogonalized U_{ij} tensor.

	x	y	z	U(eq)
Na(1)	7029(1)	2294(3)	2939(1)	26(1)
Na(2)	7978(1)	7326(3)	5913(1)	25(1)
O(1)	8151(1)	2316(5)	4472(2)	23(1)
O(2)	8331(3)	3055(11)	2544(4)	22(1)
O(2A)	8317(17)	1850(60)	2540(20)	23(5)
O(3)	6856(1)	7540(6)	6322(2)	23(1)
O(4)	6681(2)	6820(10)	4219(4)	23(1)
O(4A)	6648(13)	8190(50)	4190(20)	23(4)
C(1)	9724(1)	5706(8)	3703(3)	16(1)
C(1A)	9737(7)	-710(40)	3703(14)	18(3)
C(2)	9293(1)	4174(8)	4398(2)	14(1)
C(2A)	9296(7)	780(40)	4375(12)	19(3)
C(3)	9575(2)	3504(11)	5701(3)	17(1)
C(3A)	9572(9)	1520(60)	5693(14)	18(3)
C(4)	8536(2)	3096(11)	3748(3)	15(1)
C(4A)	8539(9)	1830(70)	3744(18)	21(5)
C(5)	5277(1)	4258(9)	3978(3)	18(1)
C(5A)	5269(7)	10720(40)	3968(11)	10(3)
C(6)	5711(1)	5789(8)	5103(2)	15(1)
C(6A)	5701(6)	9260(40)	5085(11)	13(3)
C(7)	5427(2)	6509(11)	6126(3)	18(1)
C(7A)	5425(7)	8590(50)	6125(13)	12(3)
C(8)	6469(2)	6778(11)	5215(4)	17(1)
C(8A)	6453(8)	8040(60)	5205(15)	12(4)

Table S3. Atomic coordinates ($\times 10^4$) and equivalent isotropic displacement parameters ($Å^2 \times 10^2$) for TPAK. U_{eq} is defined as one third of the trace of the orthogonalized U_{ij} tensor.

	x	y	z	U(eq)
K(1)	1107(1)	7964(1)	1616(1)	27(1)
O(1)	1481(1)	3144(4)	3354(1)	30(1)
O(2)	1738(1)	1999(3)	5328(1)	30(1)
C(1)	2174(2)	2146(4)	4454(2)	21(1)
C(2)	3638(2)	1012(4)	4743(2)	22(1)
C(3)	4442(2)	-468(5)	5893(2)	26(1)
C(4)	4212(2)	1453(5)	3853(2)	26(1)

Table S4. Atomic coordinates ($\times 10^4$) and equivalent isotropic displacement parameters ($Å^2 \times 10^2$) for TPARb. U_{eq} is defined as one third of the trace of the orthogonalized U_{ij} tensor.

	x	y	z	U(eq)
Rb(1)	1549(1)	2038(1)	6827(1)	32(1)
O(1)	2046(2)	8107(4)	3814(2)	33(1)
O(2)	2523(2)	7021(4)	5777(2)	36(1)
O(3)	434(2)	2652(6)	3962(2)	39(1)
C(1)	5335(2)	5448(6)	4026(2)	24(1)
C(2)	4267(2)	6494(6)	3946(2)	26(1)
C(3)	3913(2)	6049(5)	4916(2)	21(1)
C(4)	2749(2)	7157(5)	4841(2)	22(1)

Table S5. Selected bond lengths (Å) for TPANa.

Bond	Length	Bond	Length
Na(1)−O(4A)#1	2.252(19)	Na(1)−O(4)	2.342(4)
Na(1)−O(1)	2.3759(19)	Na(1)−O(3)#2	2.406(2)
Na(1)−O(3)#3	2.491(2)	Na(1)−O(4)#1	2.584(4)
Na(1)−O(2A)	2.70(3)	Na(1)−O(4A)	2.706(18)
Na(1)−O(2)	2.731(6)	Na(1)−C(4A)	2.872(17)
Na(2)−O(2A)#5	2.26(2)	Na(2)−O(2)#6	2.368(4)
Na(2)−O(3)	2.3746(19)	Na(2)−O(1)#4	2.442(2)
Na(2)−O(1)	2.448(2)	Na(2)−O(2)#5	2.563(4)
Na(2)−O(2A)#6	2.68(2)	Na(2)−O(4)	2.717(4)
Na(2)−O(4A)	2.79(3)	O(1)−C(4)	1.262(4)
O(1)−C(4A)	1.251(16)	O(2A)−C(4A)	1.255(17)
O(2)−C(4)	1.253(4)	O(3)−C(8A)	1.265(15)
O(3)−C(8)	1.262(4)	O(4A)−C(8A)	1.258(16)
O(4)−C(8)	1.257(4)	C(1)−C(2)	1.391(3)
C(1)−C(3)#7	1.385(4)	C(1A)−C(3A)#8	1.37(2)
C(1)−H(1)	0.9300	C(1A)−H(1A)	0.9300
C(1A)−C(2A)	1.384(15)	C(2)−C(4)	1.516(4)
C(2)−C(3)	1.386(4)	C(2A)−C(4A)	1.509(16)
C(2A)−C(3A)	1.404(15)	C(3A)−H(3A)	0.9300
C(3)−H(3)	0.9300	C(5)−C(6)	1.393(4)
C(5)−C(7)#9	1.390(4)	C(5A)−C(7A)#10	1.368(19)
C(5)−H(5)	0.9300	C(5A)−H(5A)	0.9300
C(5A)−C(6A)	1.377(14)	C(6)−C(8)	1.509(4)
C(6)−C(7)	1.393(4)	C(6A)−C(8A)	1.517(16)
C(6A)−C(7A)	1.397(14)	C(7A)−H(7A)	0.9300
C(7)−H(7)	0.9300		

Table S6. Selected bond lengths (Å) for TPAK.

Bond	Length	Bond	Length
K(1)−O(1)	2.6711(14)	K(1)−O(2)#1	2.6886(14)
K(1)−O(2)#2	2.7097(14)	K(1)−O(1)#3	2.7444(14)
K(1)−O(1)#4	2.7734(15)	K(1)−O(2)#3	2.9834(15)
O(1)−C(1)	1.252(2)	O(2)−C(1)	1.261(2)
C(1)−C(2)	1.514(3)	C(2)−C(3)	1.390(3)
C(2)−C(4)	1.391(3)	C(3)−C(4)#7	1.388(3)
C(3)−H(3)	0.9300	C(4)−H(4)	0.9300

Table S7. Selected bond lengths (Å) for TPARb.

Bond	Length	Bond	Length
Rb(1)−O(2)	2.8429(17)	Rb(1)−O(2)#1	2.8522(17)
Rb(1)−O(1)#2	2.9173(17)	Rb(1)−O(3)#3	2.975(2)
Rb(1)−O(1)#4	2.9941(18)	Rb(1)−O(3)#5	3.134(2)
Rb(1)−O(3)	3.160(2)	Rb(1)−O(3)#4	3.324(2)
O(1)−C(4)	1.266(3)	O(2)−C(4)	1.244(3)
O(3)−H(3A)	0.81(3)	O(3)−H(3B)	0.75(3)
C(1)−C(2)	1.381(3)	C(1)−C(3)#7	1.391(3)
C(1)−H(1)	0.9300	C(2)−C(3)	1.391(3)
C(2)−H(2)	0.93(3)	C(3)−C(4)	1.507(3)

Table S8. Selected bond angles (°) for TPANa.

Bond	Angle	Bond	Angle
O(4A)#1−Na(1)−O(1)	89.1(7)	O(4)−Na(1)−O(1)	87.35(11)
O(1)−Na(1)−O(3)#2	115.43(7)	O(1)−Na(1)−O(3)#3	114.22(7)
O(3)#2−Na(1)−O(3)#3	92.83(6)	O(1)−Na(1)−O(4)#1	87.85(10)
O(3)#2−Na(1)−O(4)#1	81.23(10)	O(3)#3−Na(1)−O(4)#1	157.39(11)
O(1)−Na(1)−O(2A)	51.1(5)	O(3)#2−Na(1)−O(2A)	78.2(5)
O(3)#3−Na(1)−O(2A)	83.4(5)	O(4A)#1−Na(1)−O(4A)	90.9(6)
O(1)−Na(1)−O(4A)	89.0(6)	O(3)#2−Na(1)−O(4A)	155.5(6)
O(3)#3−Na(1)−O(4A)	77.2(4)	O(1)−Na(1)−O(2)	51.05(9)
O(3)#2−Na(1)−O(2)	84.81(10)	O(3)#3−Na(1)−O(2)	76.82(9)
O(2)#6−Na(2)−O(3)	86.50(15)	O(2A)#5−Na(2)−O(3)	88.2(9)
O(3)−Na(2)−O(1)#4	113.29(7)	O(2)#6−Na(2)−O(1)#4	84.82(12)
O(2)#6−Na(2)−O(1)	155.84(14)	O(2A)#5−Na(2)−O(1)	87.5(6)
O(1)#4−Na(2)−O(1)	92.99(6)	O(3)−Na(2)−O(1)	116.14(7)
O(3)−Na(2)−O(2)#5	89.30(14)	O(2)#6−Na(2)−O(2)#5	91.94(14)
O(1)−Na(2)−O(2)#5	80.67(11)	O(1)#4−Na(2)−O(2)#5	156.86(14)
O(3)−Na(2)−O(2A)#6	86.1(7)	O(2)#6−Na(2)−O(2A)#6	6.8(5)
O(1)−Na(2)−O(2A)#6	157.7(7)	O(1)#4−Na(2)−O(2A)#6	78.9(5)
O(3)−Na(2)−O(4)	51.15(9)	O(2)#5−Na(2)−O(2A)#6	98.7(4)
O(1)−Na(2)−O(4)	78.01(9)	O(1)#4−Na(2)−O(4)	83.56(9)
O(1)#4−Na(2)−O(4A)	76.4(4)	O(3)−Na(2)−O(4A)	50.6(4)
O(3)−Na(2)−C(8)	25.64(9)	O(1)−Na(2)−O(4A)	85.6(4)
C(4)−O(1)−Na(1)	99.94(19)	C(4A)−O(1)−Na(1)	100.1(9)
Na(1)−O(1)−Na(2)#1	100.19(7)	C(4)−O(1)−Na(2)#1	140.1(2)
C(4)−O(1)−Na(2)	116.6(2)	C(4A)−O(1)−Na(2)	135.7(11)
Na(2)#1−O(1)−Na(2)	93.00(6)	Na(1)−O(1)−Na(2)	100.43(7)
C(4)−O(2)−Na(2)#2	132.3(3)	C(4)−O(2)−Na(2)#3	135.3(3)
C(4)−O(2)−Na(1)	83.6(3)	Na(2)#3−O(2)−Na(2)#2	91.94(14)
Na(2)#2−O(2)−Na(1)	86.75(14)	Na(2)#3−O(2)−Na(1)	94.98(17)
C(4A)−O(2A)−Na(1)	85.0(17)	Na(2)#2−O(2A)−Na(2)#3	91.5(7)
Na(2)#3−O(2A)−Na(1)	89.0(9)	Na(2)#2−O(2A)−Na(1)	94.1(10)
C(8A)−O(3)−Na(2)	101.6(8)	C(8)−O(3)−Na(2)	99.8(2)
Na(2)−O(3)−Na(1)#6	101.43(7)	Na(2)−O(3)−Na(1)#5	99.10(7)
C(8)−O(4)−Na(1)	135.9(3)	Na(1)#5−O(3)−Na(1)#6	92.83(6)
C(8)−O(4)−Na(2)	84.0(3)	Na(1)−O(4)−Na(1)#4	92.01(12)
Na(1)#4−O(4)−Na(2)	88.38(12)	Na(1)−O(4)−Na(2)	93.95(13)
Na(1)#4−O(4A)−Na(1)	90.9(6)	C(8A)−O(4A)−Na(1)	126.7(14)
Na(1)#4−O(4A)−Na(2)	93.7(8)	C(8A)−O(4A)−Na(2)	82.5(14)
C(3)#7−C(1)−C(2)	120.5(2)	Na(1)−O(4A)−Na(2)	84.8(6)
C(2)−C(1)−H(1)	119.7	C(3)#7−C(1)−H(1)	119.7
C(3A)#8−C(1A)−H(1A)	119.4	C(3A)#8−C(1A)−C(2A)	121.2(13)
C(3)−C(2)−C(1)	118.7(2)	C(2A)−C(1A)−H(1A)	119.4
C(1)−C(2)−C(4)	121.3(2)	C(3)−C(2)−C(4)	120.0(3)

C(1A)−C(2A)−C(4A)	123.0(13)	C(1A)−C(2A)−C(3A)	118.6(13)
C(1)#7−C(3)−C(2)	120.8(3)	C(3A)−C(2A)−C(4A)	118.4(14)
C(2)−C(3)−H(3)	119.6	C(1)#7−C(3)−H(3)	119.6
C(1A)#8−C(3A)−H(3A)	119.9	C(1A)#8−C(3A)−C(2A)	120.2(14)
O(2)−C(4)−O(1)	124.3(4)	C(2A)−C(3A)−H(3A)	119.9
O(1)−C(4)−C(2)	116.9(3)	O(2)−C(4)−C(2)	118.8(3)
O(2A)−C(4A)−C(2A)	119.6(19)	O(1)−C(4A)−C(2A)	116.7(15)
C(7)#9−C(5)−C(6)	120.6(3)	C(7)#9−C(5)−H(5)	119.7
C(6)−C(5)−H(5)	119.7	C(7A)#10−C(5A)−C(6A)	120.0(11)
C(7A)#10−C(5A)−H(5A)	120.0	C(6A)−C(5A)−H(5A)	120.0
C(5)−C(6)−C(7)	118.7(2)	C(5)−C(6)−C(8)	121.4(3)
C(7)−C(6)−C(8)	119.9(3)	C(5A)−C(6A)−C(7A)	119.0(12)
C(5A)−C(6A)−C(8A)	122.7(11)	C(7A)−C(6A)−C(8A)	118.1(12)
C(5)#9−C(7)−C(6)	120.7(3)	C(5)#9−C(7)−H(7)	119.7
C(6)−C(7)−H(7)	119.7	C(5A)#10−C(7A)−C(6A)	120.9(12)
C(5A)#10−C(7A)−H(7A)	119.5	C(6A)−C(7A)−H(7A)	119.5
O(4)−C(8)−O(3)	123.6(4)	O(4)−C(8)−C(6)	119.3(3)
O(3)−C(8)−C(6)	117.2(3)	O(3)−C(8A)−C(6A)	117.8(13)
O(4A)−C(8A)−O(3)	125.2(17)	O(4A)−C(8A)−C(6A)	116.0(15)

Symmetry transformations used to generate equivalent atoms:

#1 x,y−1,z #2 x,−y+1/2,z−1/2 #3 x,−y+3/2,z−1/2

#4 x,y+1,z #5 x,−y+1/2,z+1/2 #6 x,−y+3/2,z+1/2

#7 −x+2,−y+1,−z+1 #8 −x+2,−y,−z+1 #9 −x+1,−y+1,−z+1

#10 −x+1,−y+2,−z+1

Table S9. Selected bond angles (°) for TPAK.

Bond	Angle	Bond	Angle
O(1)−K(1)−O(2)#1	84.39(5)	O(1)−K(1)−O(2)#2	158.94(5)
O(2)#1−K(1)−O(2)#2	93.53(5)	O(1)−K(1)−O(1)#3	82.21(4)
O(2)#1−K(1)−O(1)#3	119.22(4)	O(2)#2−K(1)−O(1)#3	116.55(4)
O(1)−K(1)−O(1)#4	92.48(5)	O(2)#1−K(1)−O(1)#4	159.32(4)
O(2)#2−K(1)−O(1)#4	82.07(4)	O(1)#3−K(1)−O(1)#4	80.38(4)
O(1)−K(1)−O(2)#3	106.35(4)	O(2)#1−K(1)−O(2)#3	83.53(4)
O(2)#2−K(1)−O(2)#3	94.18(4)	O(1)#3−K(1)−O(2)#3	45.52(4)
O(1)#4−K(1)−O(2)#3	116.85(4)	C(1)−O(1)−K(1)#8	99.74(11)
C(1)−O(1)−K(1)	146.78(12)	C(1)−O(1)−K(1)#6	111.18(11)
K(1)−O(1)−K(1)#8	99.91(4)	K(1)#8−O(1)−K(1)#6	97.42(5)
K(1)−O(1)−K(1)#6	92.48(5)	C(1)−O(2)−K(1)#10	130.38(11)
C(1)−O(2)−K(1)#9	136.08(11)	C(1)−O(2)−K(1)#8	88.26(11)
K(1)#9−O(2)−K(1)#10	93.53(5)	K(1)#10−O(2)−K(1)#8	85.82(4)
K(1)#9−O(2)−K(1)#8	96.47(4)	O(1)−C(1)−C(2)	117.12(17)
O(1)−C(1)−O(2)	124.78(17)	C(3)−C(2)−C(1)	121.48(17)
O(2)−C(1)−C(2)	118.09(17)	C(4)#7−C(3)−C(2)	120.68(18)
C(3)−C(2)−C(4)	118.32(17)	C(2)−C(3)−H(3)	119.7
C(4)−C(2)−C(1)	120.20(17)	C(3)#7−C(4)−H(4)	119.5
C(4)#7−C(3)−H(3)	119.7	C(2)−C(4)−H(4)	119.5
C(3)#7−C(4)−C(2)	121.00(18)		

Symmetry transformations used to generate equivalent atoms:

#1 x,−y+1/2,z−1/2 #2 x,−y+3/2,z−1/2 #3 −x,y+1/2,−z+1/2

#4 x,y+1,z #5 −x,−y+2,−z #6 x,y−1,z #7 −x+1,−y,−z+1

#8 −x,y−1/2,−z+1/2 #9 x,−y+1/2,z+1/2 #10 x,−y+3/2,z+1/2

Table S10. Selected bond angles (°) for TPARb.

Bond	Angle	Bond	Angle
O(2)−Rb(1)−O(2)#1	87.89(5)	O(2)−Rb(1)−O(1)#2	84.18(5)
O(2)#1−Rb(1)−O(1)#2	144.11(6)	O(2)−Rb(1)−O(3)#3	138.30(6)
O(2)#1−Rb(1)−O(3)#3	83.16(6)	O(1)#2−Rb(1)−O(3)#3	124.47(6)
O(2)−Rb(1)−O(1)#4	144.63(6)	O(2)#1−Rb(1)−O(1)#4	82.63(5)
O(1)#2−Rb(1)−O(1)#4	83.90(5)	O(3)#3−Rb(1)−O(1)#4	74.28(6)
O(2)−Rb(1)−O(3)#5	80.51(6)	O(2)#1−Rb(1)−O(3)#5	139.79(6)
O(1)#2−Rb(1)−O(3)#5	73.02(6)	O(3)#3−Rb(1)−O(3)#5	80.58(5)
O(1)#4−Rb(1)−O(3)#5	126.83(6)	O(2)−Rb(1)−O(3)	64.57(6)
O(2)#1−Rb(1)−O(3)	71.23(6)	O(1)#2−Rb(1)−O(3)	133.72(5)
O(3)#3−Rb(1)−O(3)	74.00(7)	O(1)#4−Rb(1)−O(3)	140.77(5)
O(3)#5−Rb(1)−O(3)	69.00(7)	O(2)−Rb(1)−O(3)#4	133.05(5)
O(2)#1−Rb(1)−O(3)#4	137.01(5)	O(1)#2−Rb(1)−O(3)#4	52.23(5)
O(3)#3−Rb(1)−O(3)#4	73.42(6)	O(1)#4−Rb(1)−O(3)#4	56.76(5)
O(3)#5−Rb(1)−O(3)#4	71.49(6)	O(3)−Rb(1)−O(3)#4	131.86(7)
C(4)−O(1)−Rb(1)#9	114.83(13)	C(4)−O(1)−Rb(1)#8	146.39(16)
C(4)−O(2)−Rb(1)	134.39(15)	Rb(1)#8−O(1)−Rb(1)#9	83.90(5)
Rb(1)−O(2)−Rb(1)#6	87.88(5)	C(4)−O(2)−Rb(1)#6	129.62(14)
Rb(1)#3−O(3)−Rb(1)	106.00(7)	Rb(1)#3−O(3)−Rb(1)#5	80.58(5)
Rb(1)#3−O(3)−Rb(1)#9	109.35(7)	Rb(1)#5−O(3)−Rb(1)	111.00(7)
Rb(1)−O(3)−Rb(1)#9	132.30(7)	Rb(1)#5−O(3)−Rb(1)#9	105.55(7)
Rb(1)#5−O(3)−H(3A)	164(2)	Rb(1)#3−O(3)−H(3A)	94(2)
Rb(1)#9−O(3)−H(3A)	62(2)	Rb(1)−O(3)−H(3A)	84(2)
Rb(1)#5−O(3)−H(3B)	80(3)	Rb(1)#3−O(3)−H(3B)	159(3)
Rb(1)#9−O(3)−H(3B)	68(2)	Rb(1)−O(3)−H(3B)	89(2)
C(2)−C(1)−C(3)#7	120.8(2)	H(3A)−O(3)−H(3B)	103(4)
C(3)#7−C(1)−H(1)	119.6	C(2)−C(1)−H(1)	119.6
C(1)−C(2)−H(2)	117.1(18)	C(1)−C(2)−C(3)	120.8(2)
C(1)#7−C(3)−C(4)	120.1(2)	C(3)−C(2)−H(2)	122.1(18)
O(2)−C(4)−O(1)	123.8(2)	C(1)#7−C(3)−C(2)	118.4(2)
O(1)−C(4)−C(3)	117.6(2)	C(2)−C(3)−C(4)	121.5(2)
O(2)−C(4)−C(3)	118.6(2)		

Symmetry transformations used to generate equivalent atoms:

#1 x,y−1,z #2 x,−y+3/2,z+1/2 #3 −x,−y,−z+1

#4 x,−y+1/2,z+1/2 #5 −x,−y+1,−z+1 #6 x,y+1,z

#7 −x+1,−y+1,−z+1 #8 x,−y+3/2,z−1/2 #9 x,−y+1/2,z−1/2

Table S11. Anisotropic displacement parameters ($Å^2 \times 10^3$) for TPANa.

	U^{11}	U^{22}	U^{33}	U^{23}	U^{13}	U^{12}
Na(1)	22(1)	33(1)	21(1)	−4(1)	4(1)	0(1)
Na(2)	22(1)	30(1)	23(1)	−3(1)	9(1)	−1(1)
O(1)	16(1)	32(1)	22(1)	0(1)	7(1)	−4(1)
O(2)	19(1)	29(2)	16(1)	1(1)	−1(1)	−3(2)
O(2A)	29(7)	24(9)	17(6)	0(6)	9(5)	1(8)
O(3)	16(1)	32(1)	19(1)	0(1)	2(1)	−1(1)
O(4)	18(1)	31(2)	23(1)	−2(2)	10(1)	−2(2)
O(4A)	30(7)	22(8)	22(6)	3(6)	14(5)	11(7)
C(1)	16(1)	19(1)	14(1)	1(1)	3(1)	−2(1)
C(1A)	19(4)	18(4)	17(4)	0(2)	5(2)	0(2)
C(2)	12(1)	13(1)	16(1)	−2(1)	4(1)	0(1)
C(2A)	19(4)	19(4)	18(4)	1(2)	5(2)	1(2)
C(3)	16(1)	20(2)	18(1)	0(1)	7(1)	−4(1)
C(3A)	23(7)	16(7)	15(6)	−3(6)	6(5)	−7(6)
C(4)	12(1)	15(2)	18(2)	−1(1)	3(1)	2(1)
C(4A)	20(7)	17(8)	22(7)	1(6)	0(5)	1(6)
C(5)	18(1)	22(2)	16(1)	0(1)	7(1)	−1(1)
C(5A)	20(6)	7(5)	6(5)	0(4)	7(4)	−1(4)
C(6)	13(1)	14(1)	17(1)	2(1)	3(1)	0(1)
C(6A)	16(5)	10(5)	14(5)	−4(4)	4(4)	0(4)
C(7)	17(1)	21(2)	16(1)	−1(1)	4(1)	−3(1)
C(7A)	12(6)	12(6)	11(6)	5(6)	1(4)	−5(5)
C(8)	16(2)	14(2)	21(2)	1(1)	5(1)	2(1)
C(8A)	10(6)	13(8)	15(6)	1(6)	5(5)	3(5)

Table S12. Anisotropic displacement parameters ($Å^2 \times 10^3$) for TPAK.

	U^{11}	U^{22}	U^{33}	U^{23}	U^{13}	U^{12}
K(1)	28(1)	28(1)	28(1)	1(1)	15(1)	0(1)
O(1)	23(1)	40(1)	27(1)	7(1)	9(1)	6(1)
O(2)	28(1)	38(1)	30(1)	3(1)	18(1)	4(1)
C(1)	21(1)	19(1)	26(1)	−1(1)	12(1)	−1(1)
C(2)	20(1)	21(1)	25(1)	−2(1)	10(1)	−1(1)
C(3)	26(1)	34(1)	25(1)	4(1)	16(1)	2(1)
C(4)	24(1)	34(1)	20(1)	5(1)	8(1)	4(1)

Table S13. Anisotropic displacement parameters ($Å^2 \times 10^3$) for TPARb.

	U^{11}	U^{22}	U^{33}	U^{23}	U^{13}	U^{12}
Rb(1)	36(1)	33(1)	31(1)	−3(1)	15(1)	−2(1)
O(1)	20(1)	49(1)	27(1)	3(1)	4(1)	10(1)
O(2)	30(1)	49(1)	35(1)	8(1)	20(1)	10(1)
O(3)	24(1)	38(1)	54(2)	−2(1)	12(1)	1(1)
C(1)	21(1)	33(1)	19(1)	1(1)	10(1)	2(1)
C(2)	22(2)	33(1)	17(1)	3(1)	3(1)	2(1)
C(3)	19(1)	21(1)	20(1)	−1(1)	5(1)	−1(1)
C(4)	21(1)	20(1)	27(2)	−3(1)	10(1)	−3(1)

Table S14. Hydrogen coordinates ($\times 10^4$) and isotropic displacement parameters ($Å^2 \times 10^3$) for TPANa.

	x	y	z	U(eq)
H(1)	9541	6205	2831	20
H(1A)	9563	-1177	2827	22
H(3)	9291	2514	6180	21
H(3A)	9285	2564	6159	22
H(5)	5460	3744	3289	22
H(5A)	5449	11246	3276	12
H(7)	5711	7513	6886	22
H(7A)	5717	7658	6890	15

Table S15. Hydrogen coordinates ($\times 10^4$) and isotropic displacement parameters ($Å^2 \times 10^3$) for TPAK.

	x	y	z	U(eq)
H(3)	4075	−800	6499	31
H(4)	3687	2424	3076	31

Table S16. Hydrogen coordinates ($\times 10^4$) and isotropic displacement parameters ($Å^2 \times 10^3$) for TPARb.

	x	y	z	U(eq)
H(1)	5554	5749	3365	29
H(3A)	890(30)	1190(80)	3970(30)	47(10)
H(3B)	770(30)	4240(80)	4000(30)	51(11)
H(2)	3800(30)	7500(60)	3220(30)	26(7)

Table S17. The relationships between birefringence (Δ*n*) and dihedral angles (ϑ) of TPA unit to lattice plane ($\Delta\vartheta$ is defined as the difference between the maximum and minimum values of ϑ).

Material	ϑ_{TPA}	ϑ_{100}	ϑ_{010}	ϑ_{001}	$\Delta\vartheta$	Refractive index order	Calculated Δn @546 nm
TPANa	45.559	75.524	22.779	69.348	52.745	$n_{100}>n_{001}>n_{010}$	0.54
TPAK	50.206	70.957	25.103	67.833	45.854	$n_{100}>n_{001}>n_{010}$	0.45
TPARb	51.842	68.329	25.921	69.225	43.304	$n_{001}>n_{100}>n_{010}$	0.37

Table S18. Thermal stability and birefringence information of some reported organic-inorganic hybrid alkali/alkaline earth metal salts.

Number	Compounds	Birefringence	Temperature (℃)	References
1	$K_4(HC_3N_3S_3)2{\cdot}H_2O$	0.402@550 nm	101.85	[10]
2	$Cs_3Cl(HC_3N_3S_3)$	0.6@550 nm	296.85	[11]
3	$CsH_2C_6N_9{\cdot}H_2O$	0.55@550 nm	105.85	[12]
4	$Li_2(H_2C_4N_2O_3){\cdot}2H_2O$	0.218@546 nm	159.85	[13]
5	$Ba_2Ca(C_3N_3O_3)_2$	0.346@800 nm	189	[14]
6	$[LiNO_3{\cdot}H_2O{\cdot}4HP]{\cdot}4HP$	0.376@546 nm	100	[15]
7	$[Mg(NO_3)_2{\cdot}6H_2O]{\cdot}(4HP)_2$	0.522@546 nm	100	[15]
8	$Cs_3Na(H_2C_3N_3O_3)_4{\cdot}3H_2O$	0.29@514 nm	100	[16]
9	$Rb_2HCO_3F{\cdot}B(OH)_3$	0.116@546 nm	113	[17]
10	$Rb_2C_2O_4{\cdot}B(OH)_3$	0.195@546nm	113	[17]
11	$KC_9H_5O_6(H_2O)$	0.372@550 nm	80	[18]
12	$KLi(HC_3N_3O_3){\cdot}2H_2O$	0.186@514 nm	125	[19]
13	$Rb_3[C_6N_7(NCN)_3]{\cdot}3H_2O$	0.619@546 nm	76.85	[20]
14	$Cs_3[C_6N_7(NCN)_3]{\cdot}3H_2O$	0.589@546 nm	96.85	[20]
15	$Li_2Ca(H_2C_3N_3O_3)_4{\cdot}6H_2O$	0.407@800 nm	200	[21]
16	$Na_2Ba(H_2C_3N_3O_3)_4{\cdot}6H_2O$	0.389@800 nm	200	[21]
17	$Cs_2Mg(NH_2SO_3)_4{\cdot}4H_2O$	0.054@546 nm	65	[22]
18	$K_2Ca(NH_2SO_3)_4$	0.035@546 nm	205	[22]
19	$Rb_2Ca(NH_2SO_3)_4$	0.036@546 nm	205	[22]
20	$Zn_5(OH)_4(C_3N_3O_3)_2$	0.318@400 nm	562.85	[23]
21	$MgZn_4(OH)_4(C_3N_3O_3)_2$	0.316@400 nm	596.85	[23]
22	$RbNH_4(H_2C_3N_3O_3)_2{\cdot}2H_2O$	0.40@550 nm	100	[24]
23	$KBr{\cdot}H_3C_3N_3O_3$	0.273@800 nm	400	[25]
24	$Cs_2Mg(H_2C_3N_3S_3)_4{\cdot}8H_2O$	0.580@800 nm	100	[26]
25	$K_2HC_3N_3S_3{\cdot}1.5H_2O$	0.31@550 nm	196.85	[26]
26	$K_{0.5}In_{0.5}(H_2C_6N_7O_3)_2{\cdot}9H_2O$	0.35@1064 nm	102	[27]
27	$K(H_3C_3N_3O_3)(NO_3)$	0.253@546 nm	319.8	[28]
28	$Rb(H_3C_3N_3O_3)(NO_3)$	0.224@546 nm	324.4	[28]
29	$Na[B_3O_3F_2(OH)_2]{\cdot}[B(OH)_3]$	0.1252@546 nm	193	[29]
30	**TPANa**	**0.54@550nm**	**580**	**This work**
31	**TPAK**	**0.45@550nm**	**580**	**This work**

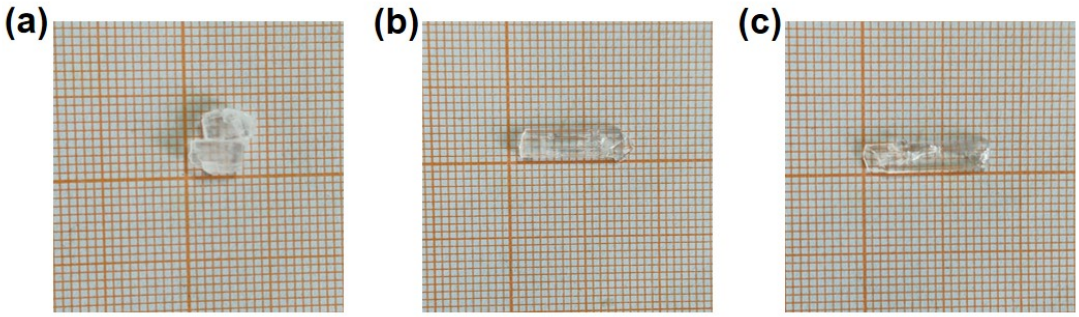

Fig. S1. Photographs of the crystals of TPANa (a), TPAK (b), TPARb (c) synthesized by hydrothermal method.

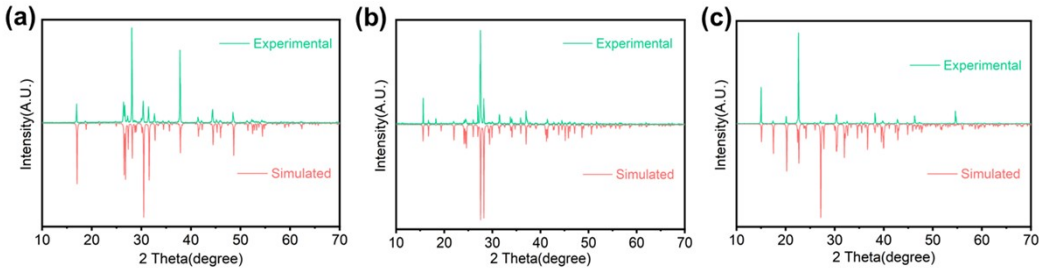

Fig. S2. Experimental and calculated XRD patterns of TPANa (a), TPAK (b), TPARb (c).

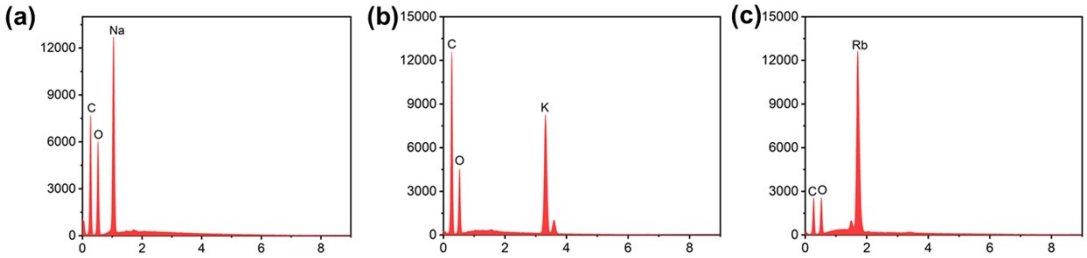

Fig. S3. Energy-dispersive X-ray (EDX) spectrometry plots of TPANa (a), TPAK (b), TPARb (c).

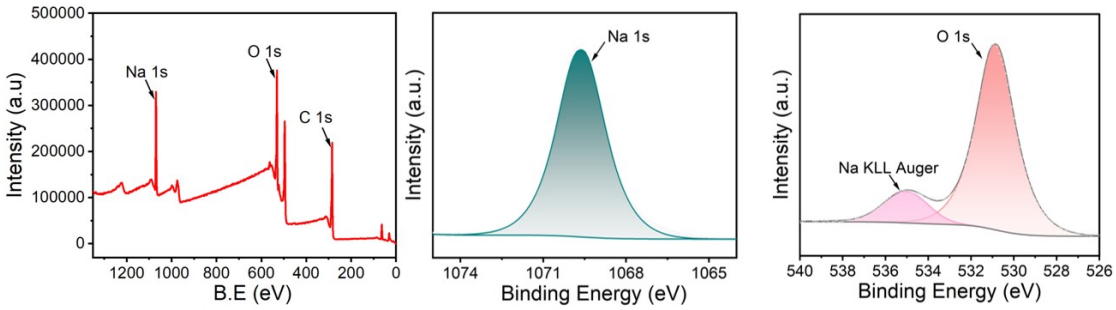

Fig. S4. XPS spectra and fitting results for TPANa.

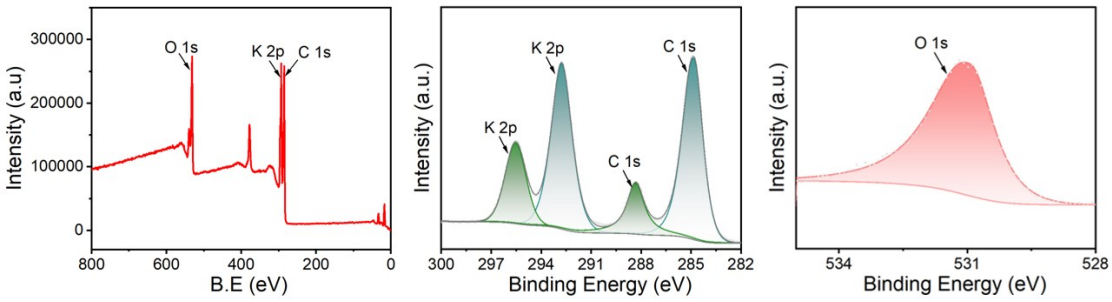

Fig. S5. XPS spectra and fitting results for TPAK.

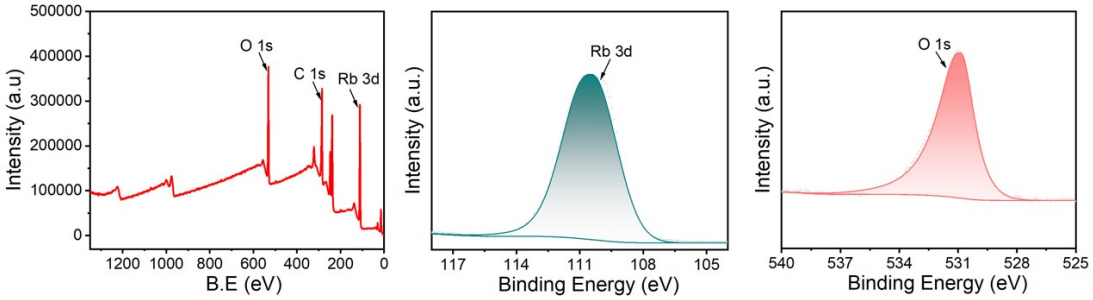

Fig. S6. XPS spectra and fitting results for TPARb.

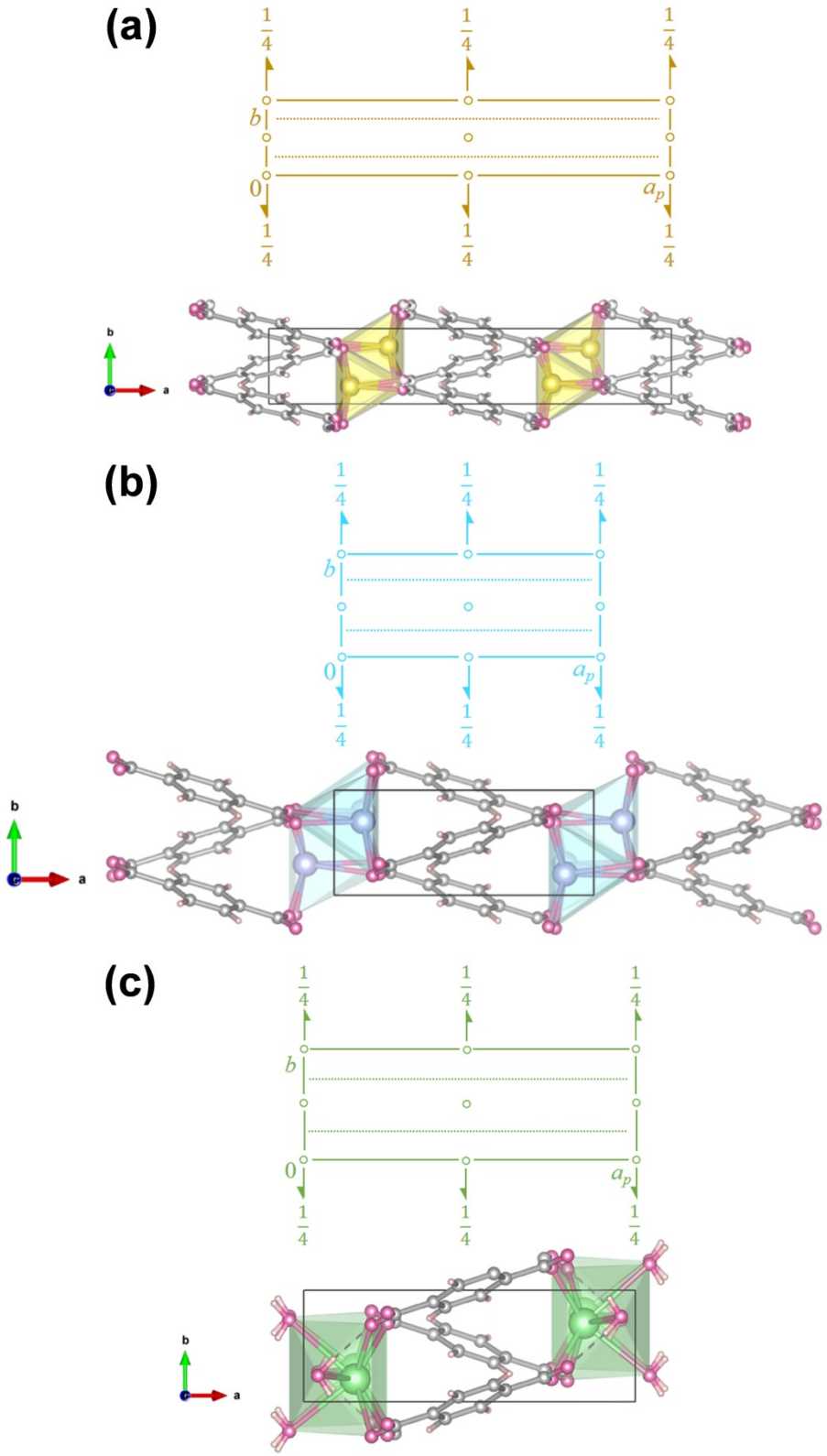

Fig. S7. Symmetrical elements diagrams and the unit cell contents of the structures of TPANa (a), TPAK (b), TPARb (c).

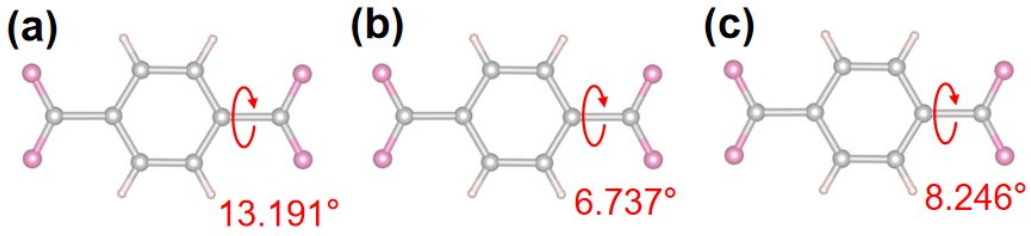

Fig. S8. The twist angle between the carboxyl and benzene ring in the structures of TPANa (a), TPAK (b), TPARb (c).

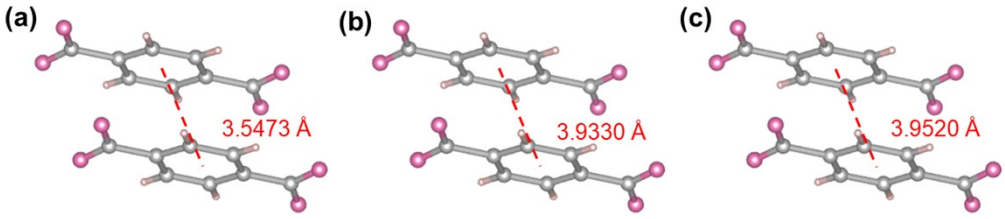

Fig. S9. The π-π stacking interactions of TPA molecules in TPANa (a), TPAK (b), TPARb (c).

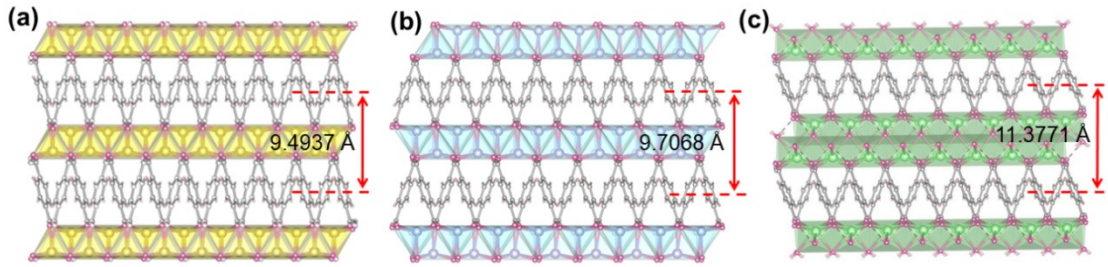

Fig. S10. The organic layer spacing of TPANa (a), TPAK (b), TPARb (c).

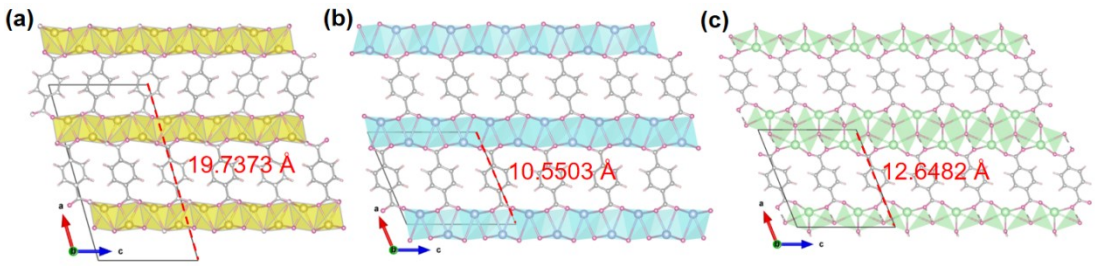

Fig. S11. The structures of TPANa (a), TPAK (b), TPARb (c) viewed along the *b*-axis.

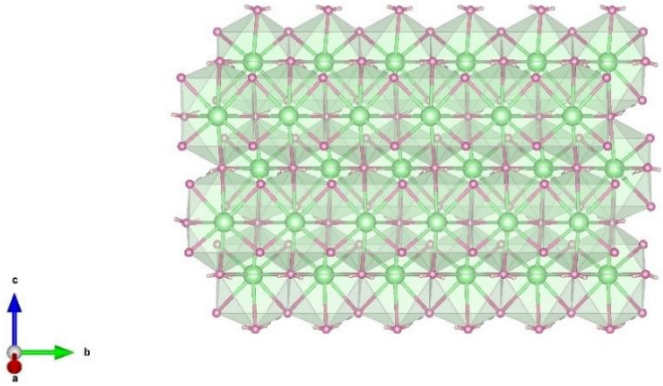

Fig. S12. $[RbO_{4/2}(H_2O)_{4/4}]_\infty$ layer in TPARb structure viewed along the direction perpendicular to the *bc*-plane.

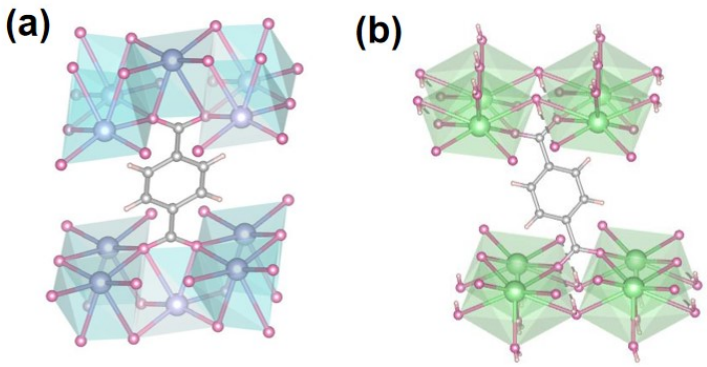

Fig. S13. The coordination environments of the TPA in TPAK (a) and TPARb (b) structures.

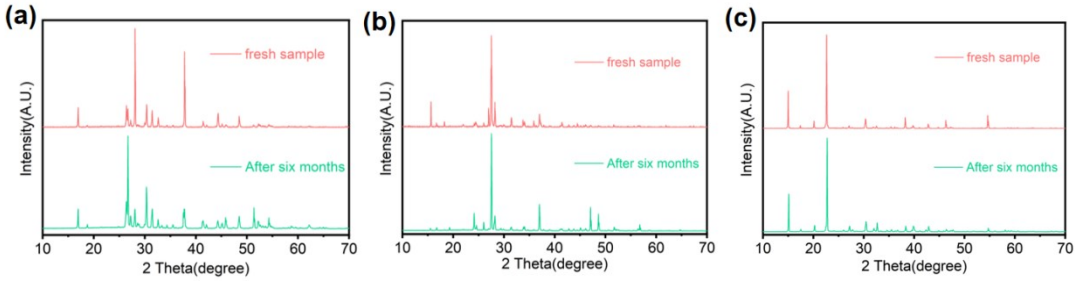

Fig. S14. Experimental powder XRD patterns of fresh samples and that the samples after exposing for six months for TPANa (a), TPAK (b), TPARb (c).

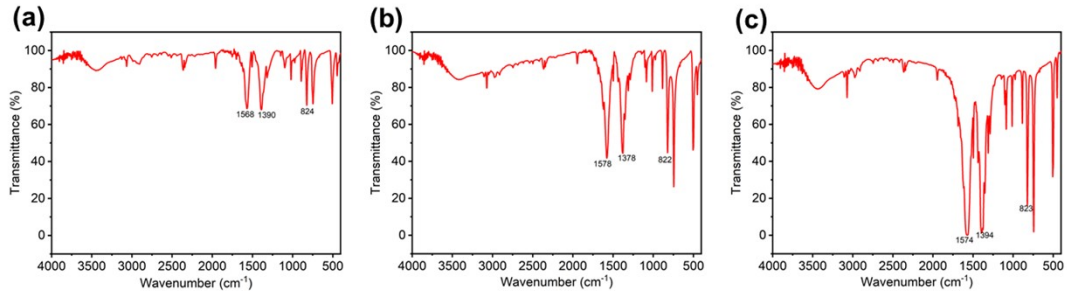

Fig. S15. IR spectra of TPANa (a), TPAK (b), TPARb (c).

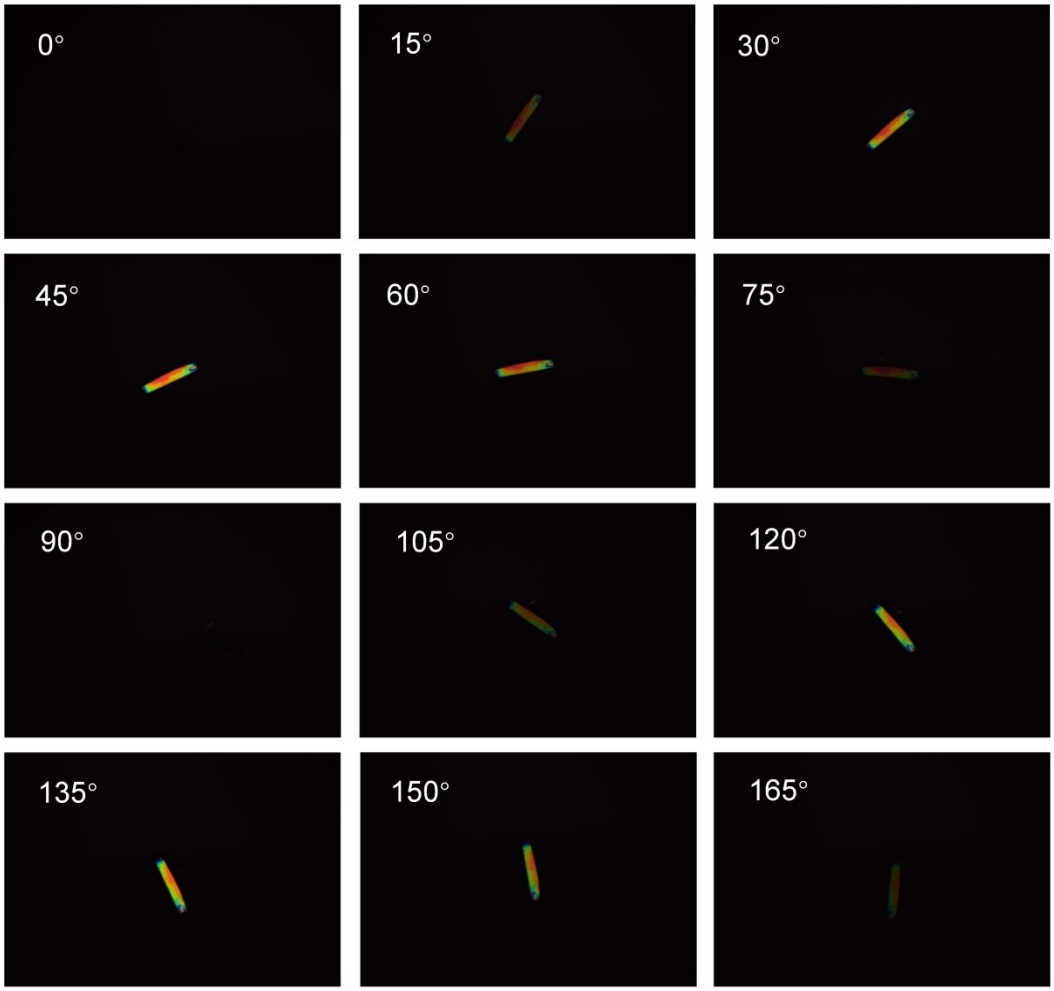

Fig. S16. Optical images of a TPANa single crystal irradiated by orthogonally polarized light at different rotation angles. The angle ϑ = 0° was defined by the moment that the crystal exhibits complete extinction.

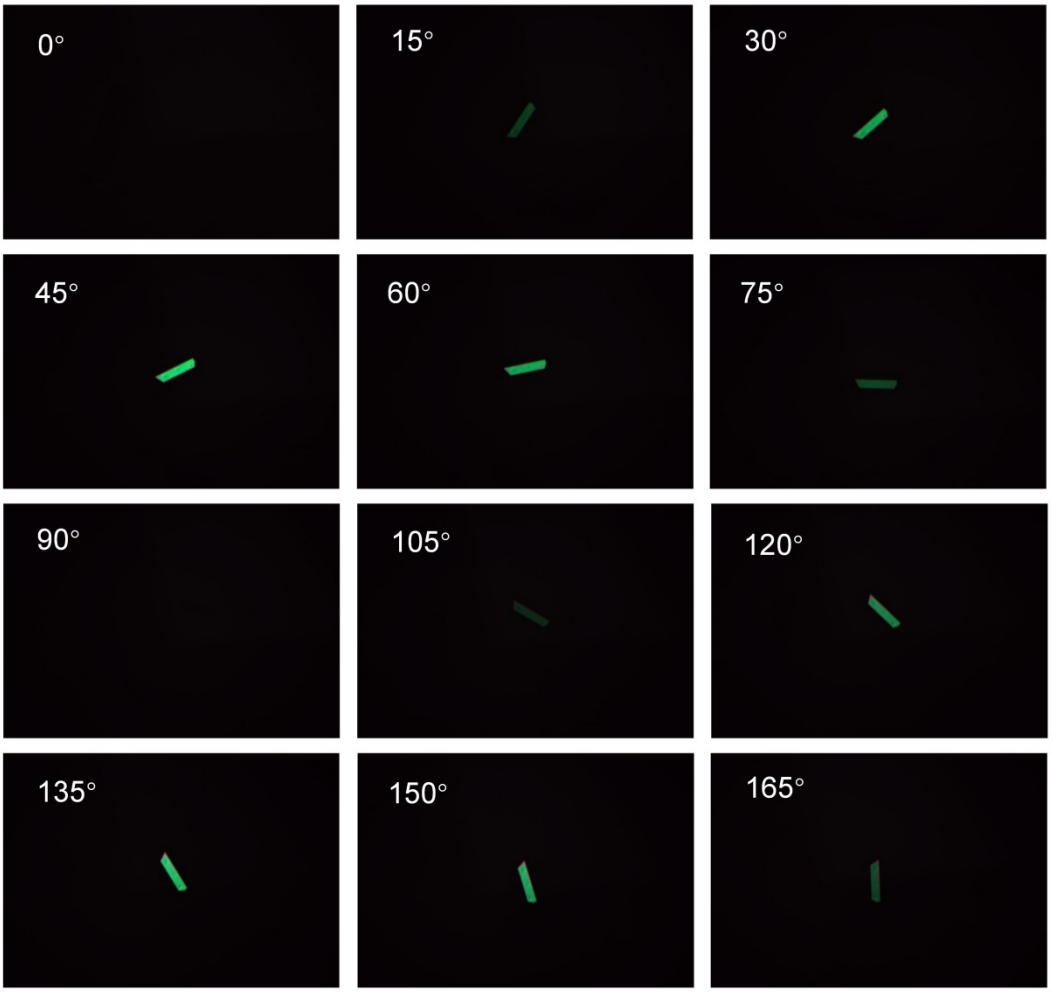

Fig. S17. Optical images of a TPAK single crystal irradiated by orthogonally polarized light at different rotation angles. The angle ϑ = 0° was defined by the moment that the crystal exhibits complete extinction.

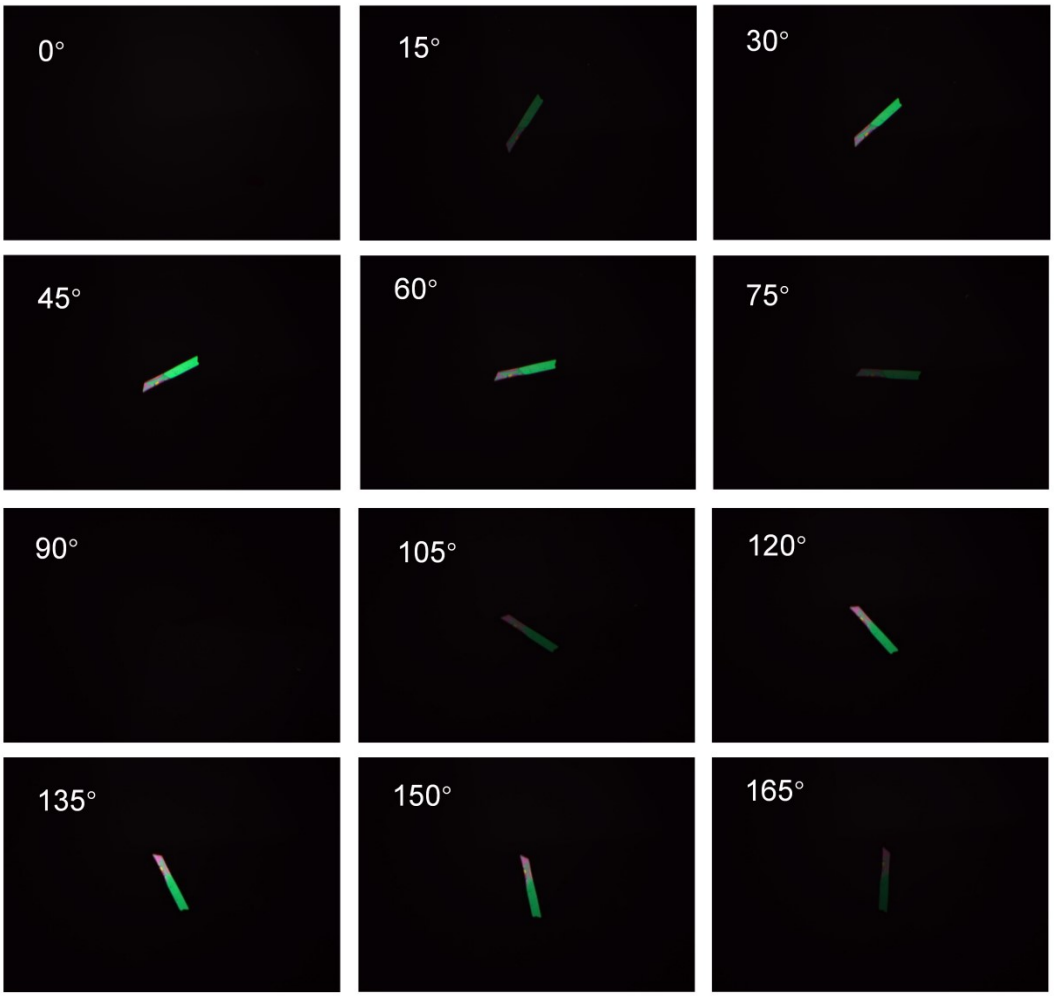

Fig. S18. Optical images of a TPARb single crystal irradiated by orthogonally polarized light at different rotation angles. The angle ϑ = 0° was defined by the moment that the crystal exhibits complete extinction.

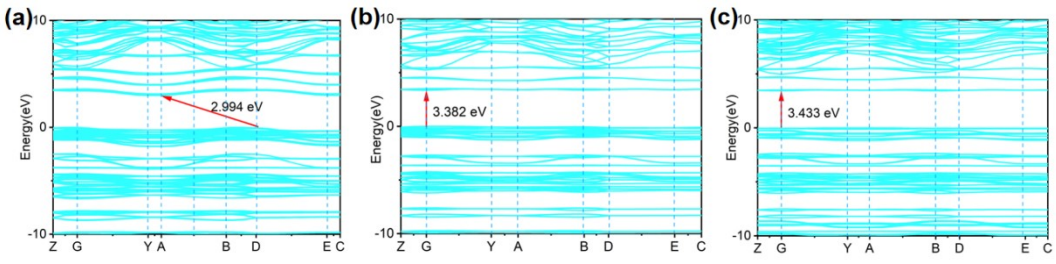

Fig. S19. The calculated band structures of TPANa (a), TPAK (b), TPARb (c).

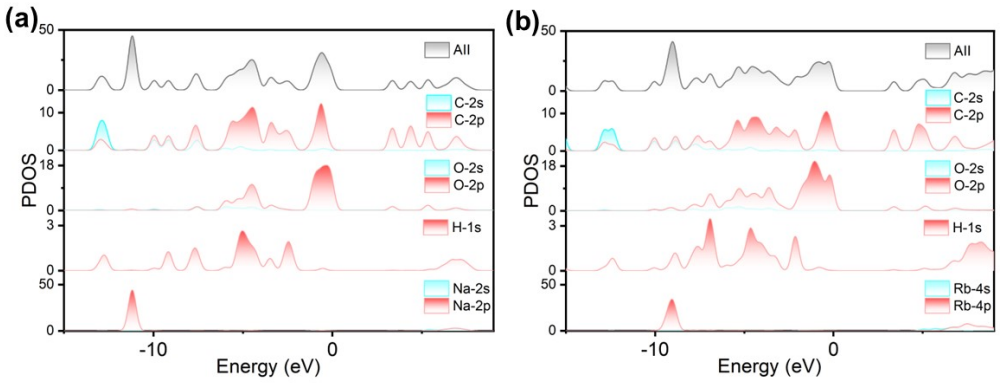

Fig. S20. Density of states diagrams of TPANa (a) and TPARb (b).

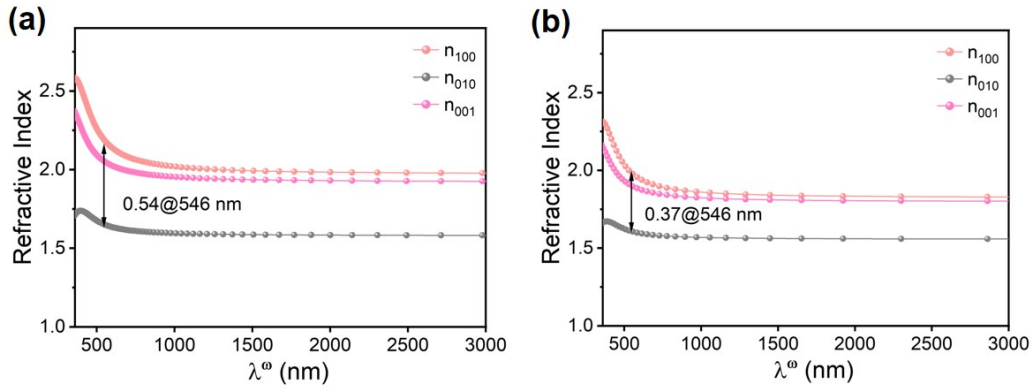

Fig. S21. Calculated refractive index dispersion curves of TPANa (a) and TPARb (b).

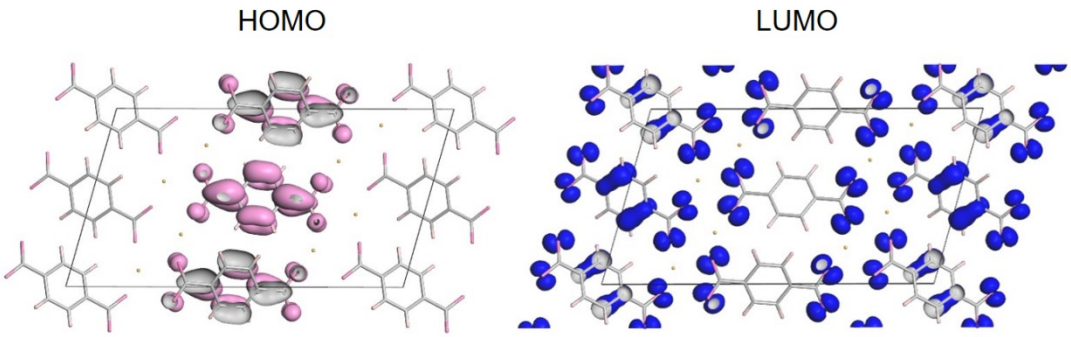

Fig. S22. The HOMO and LUMO electron cloud density maps of TPANa.

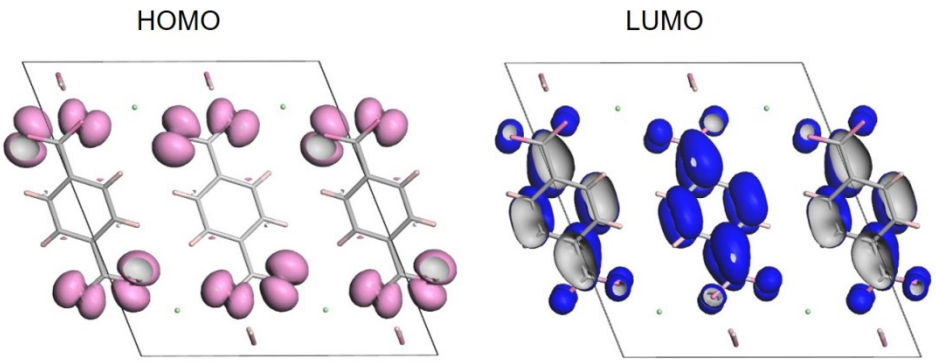

Fig. S23. The HOMO and LUMO electron cloud density maps of TPARb.

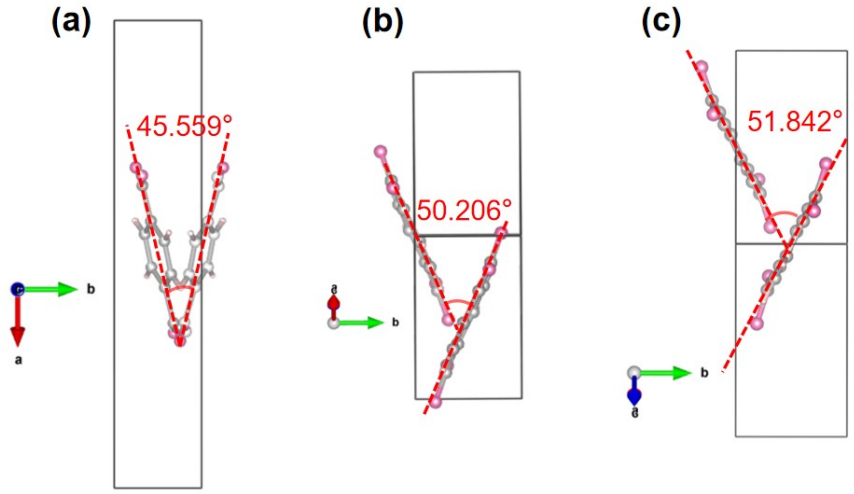

Fig. S24. The ϑ_{TPA} in the structures of TPANa (a), TPAK (b), TPARb (c).

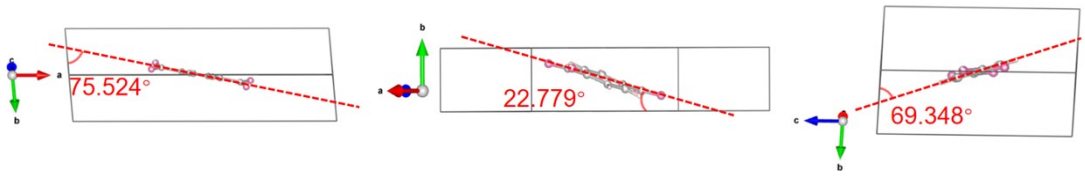

Fig. S25. The dihedral angles of TPA unit to the lattice planes of (100), (010), and (001) in TPANa.

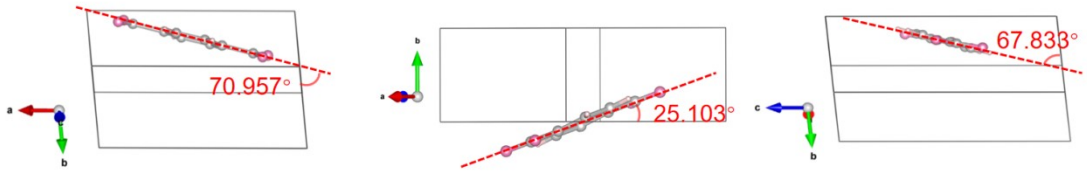

Fig. S26. The dihedral angles of TPA unit to the lattice planes of (100), (010), and (001) in TPAK.

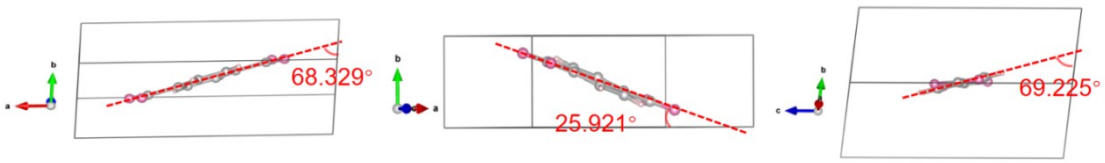

Fig. S27. The dihedral angles of TPA unit to the lattice planes of (100), (010), and (001) in TPARb.

3. References:

1 P. A. Wilks, Reflection measurements: reflectance spectroscopy. By wesley wm. Wendlandt and harry g. Hecht. Interscience (wiley), new york, 1966. 306 pp., Illus. $12., *Science*, 1966, **154**, 143.

2 B. E. Sørensen, A revised michel-lévy interference colour chart based on first-principles calculations, *Eur. J. Mineral.*, 2012, **25**, 5-10.

3 G. M. Sheldrick, A short history of*SHELX*, *Acta Crystallogr. C.*, 2008, **64**, 112-122.

4 O. V. Dolomanov, L. J. Bourhis, R. J. Gildea, J. A. K. Howard and H. Puschmann, *OLEX2* : a complete structure solution, refinement and analysis program, *J. Appl. Crystallogr.*, 2009, **42**, 339-341.

5 A. L. Spek, Single-crystal structure validation with the program PLATON, *J. Appl. Crystallogr.*, 2003, **36**, 7-13.

6 S. J. Clark, M. D. Segall, C. J. Pickard, P. J. Hasnip, M. I. J. Probert, K. Refson and M. C. Payne, First principles methods using CASTEP, *Z. Krist.Cryst. Mater*., 2005, **220**, 567-570.

7 M. P. Teter, D. C. Allan, T. A. Arias, J. D. Joannopoulos and M. C. Payne, Iterative minimization techniques for ab initio total-energy calculations: molecular dynamics and conjugate gradients, *Rev. Mod. Phys.*, 1992, **64**, 1045-1097.

8 L. J. Sham and W. Kohn, Self-consistent equations including exchange and correlation effects, *Phys. Rev*., 1965, **140**, A1133-A1138.

9 J. D. Pack and H. J. Monkhorst, Special points for brillouin-zone integrations, *Phys. Rev. B*, 1976, **13**, 5188-5192.

10 Q. Xu, Y. Liu, Q. Wu, L. Hou, Y. Li, L. Li, Z. Lin, S. Zhao and J. Luo, *α*-BBO-like trithiocyanate with significantly enhanced birefringence and second-harmonic generation, *Sci. China Mater*., 2023, **66**, 3271-3277.

11 M. Li, X. Zhang, Z. Xiong, Y. Li, Y. Zhou, X. Chen, Y. Song, M. Hong, J. Luo and S. Zhao, A hybrid antiperovskite with strong linear and second-order nonlinear optical responses, *Angew. Chem., Int. Ed.*, 2022, **61**, e202211151.

12 Y. Li, X. Zhang, Y. Zhou, W. Huang, Y. Song, H. Wang, M. Li, M. Hong, J. Luo and S. Zhao, An optically anisotropic crystal with large birefringence arising from cooperative π orbitals, *Angew. Chem., Int. Ed.*, 2022, **134**, e202208811.

13 D. Lin, M. Luo, C. Lin, L. Cao and N. Ye, An optimal arrangement of $(H_2C_4N_2O_3)^{2-}$ groups in the first non-centrosymmetric alkali barbiturate $Li_2(H_2C_4N_2O_3)\cdot 2H_2O$ inducing a giant second harmonic generation response and a striking birefringence, *Cryst. Growth Des.*, 2020, **20**, 4904-4908.

14 Z. Li, F. Liang, Y. Guo, Z. Lin, J. Yao, G. Zhang, W. Yin, Y. Wu and C. Chen, $Ba_2M(C_3N_3O_3)_2$ (M = Mg, Ca): potential UV birefringent materials with strengthened optical anisotropy originating from the $(C_3N_3O_3)^{3-}$ group, *J. Mater. Chem. C*, 218, **6**, 12879-12887.

15 Y. Li and K. M. Ok, Crystal clear: unveiling giant birefringence in organic–inorganic cocrystals, *Chem. Sci.*, 2024, **15**, 10193-10199.

16 X. Meng, F. Liang, J. Tang, K. Kang, Q. Huang, W. Yin, Z. Lin and M. Xia, $Cs_3Na(H_2C_3N_3O_3)_4\cdot 3H_2O$: a mixed alkali-metal hydroisocyanurate nonlinear optical material containing π-conjugated six-membered-ring units, *Eur. J. Inorg. Chem.*, 2019, **2019**, 2791-2795.

17 G. Xu, C. Hu, H. Li, J. Lu, Z. Yang, J. Han and S. Pan, Improving the performance of birefringent crystals by molecular assembly strategy in the solar-blind UV region, *Small*, 2025, **21**, 2504184.

18 S. Li, L. Hu, R. Tang, Y. Ma, F. Mao, J. Zheng, X. Zhang and D. Yan, $KC_9H_5O_6(H_2O)$: a promising UV nonlinear-optical material with large birefringence based on a π-conjugated $(C_9H_5O_6)^-$ group, *Inorg. Chem.*, 2022, **61**, 14880-14886.

19 D. Lin, M. Luo, C. Lin, F. Xu and N. Ye, $KLi(HC_3N_3O_3)\cdot 2H_2O$: solvent-drop grinding method toward the hydro-isocyanurate nonlinear optical crystal, *J. Am. Chem. Soc.*, 2019, **141**, 3390-3394.

20 D. Dou, B. Zhang, D. Yang and Y. Wang, Large second harmonic generation and birefringence from extended octupolar π-conjugated structures, *Chem. Sci.*, 2024, **15**, 19496-19503.

21 X. Meng, F. Liang, J. Tang, K. Kang, W. Yin, T. Zeng, B. Kang, Z. Lin and M. Xia, LiO_4 tetrahedra lock the alignment of π-conjugated layers to maximize optical anisotropy in metal hydroisocyanurates, *Inorg. Chem. Front.*, 2019, **6**, 2850-2854.

22 X. Wang, X. Leng, Y. Kuk, J. Lee, Q. Jing and K. M. Ok, Deep-ultraviolet transparent mixed metal sulfamates with enhanced nonlinear optical properties and birefringence, *Angew. Chem., Int. Ed.*, 2024, **63**, e202315434.

23 X. Liu, P. Gong and Z. Lin, $AZn_4(OH)_4(C_3N_3O_3)_2$ (A = Mg, Zn): two Zn-based cyanurate crystals with various cation coordination and large birefringence, *Inorg. Chem.*, 2021, **60**, 10890-10894.

24 M. Aibibula and L. Wang, A UV birefringent crystal: $RbNH_4(H_2C_3N_3O_3)_2{\cdot}2H_2O$, *Inorg. Chem. Commun.*, 2020, **120**, 108149.

25 X. Meng, K. Kang, Y. Liu, J. Tang, X. Jiang, W. Yin, Z. Lin and M. Xia, Mechanochemical synthesis of an ionic cocrystal with large birefringence resulting from neutral planar π-conjugated groups, *Cryst. Growth Des.*, 2020, **20**, 7588-7592.

26 Y. Song, W. Huang, Y. Zhou, Y. Li, Q. Xu, H. Wang, M. Li, X. Kuang, J. Luo and S. Zhao, *α*-BBO-like π-conjugated crystal with large birefringence, *Cryst. Growth Des.*, 2023, **23**, 1330-1335.

27 L. Zhang, F. Wang, X. Zhang, F. Liang, Z. Hu and Y. Wu, Synthesis and characterization of metal iso-cyamelurate $K_{0.5}In_{0.5}(H_2C_6N_7O_3)_2{\cdot}9H_2O$ with large birefringence, *Cryst. Growth Des.*, 2024, **24**, 627-631.

28 X. Hao, M. Luo, C. Lin, G. Peng, T. Yan, D. Lin, L. Cao, X. Long, G. Yang and N. Ye, $A(H_3C_3N_3O_3)(NO_3)$ (A = K, Rb): alkali-metal nitrate isocyanurates with strong optical anisotropy, *Inorg. Chem.*, 2020, **59**, 10361-10367.

29 C. Jin, X. Shi, H. Zeng, S. Han, Z. Chen, Z. Yang, M. Mutailipu and S. Pan, Hydroxyfluorooxoborate $Na[B_3O_3F_2(OH)_2]{\cdot}[B(OH)_3]$: optimizing the optical anisotropy with heteroanionic units for deep ultraviolet birefringent crystals, *Angew. Chem., Int. Ed.*, 2021, **133**, 20632-20638.